A Particle Filter-based Adaptive Inflation Scheme for the Ensemble Kalman Filter

A Particle Filter-based Adaptive Inflation Scheme for the Ensemble Kalman Filter

Boujemaa Ait-El-Fquih* and Ibrahim Hoteit

King Abdullah University of Science and Technology (KAUST), Thuwal, Saudi Arabia

*Correspondence to: Boujemaa Ait-El-Fquih, KAUST 4700, 23955-6900 Thuwal, Saudi Arabia.

E-mail: boujemaa.aitelfquih@kaust.edu.sa

An adaptive covariance inflation scheme is proposed for the ensemble Kalman filter (EnKF) to mitigate for the loss of ensemble variance. Adaptive inflation methods are mostly based on a Bayesian approach, which considers the inflation factor as a random variable with a given prior probability distribution, and then combines it with the inflation likelihood through Bayes' rule to obtain its posterior distribution. In this work, we introduce a numerical implementation of this generic Bayesian approach that uses a particle filter (PF) to compute a Monte Carlo approximation of the inflation posterior distribution. To alleviate the sample attrition issue, the proposed PF employs an artificial dynamical model for the inflation factor based on the well-known smoothing-kernel West and Liu model. The positivity constraint on the inflation factor is further imposed through an inverse-Gamma transition density, whose parameters suggest analytical expressions. The resulting PF-EnKF scheme is straightforward to implement, and can use different number of particles in its EnKF and PF components. Numerical experiments are conducted with the Lorenz-96 model to demonstrate the effectiveness of the proposed method under various experimental scenarios.

Key Words: Data assimilation; Adaptive inflation; Ensemble Kalman filter; Particle filter.

Received . . .

1. Introduction

Data assimilation combines observations and dynamical models to determine "best" estimates of geophysical states of interest (Reichle 2008; Edwards *et al.* 2015; Hoteit *et al.* 2018). Nowadays, data assimilation is a well-established field with a broad range of Bayesian estimation methods that can be classified into two groups: variational (optimization) methods that seek to maximize the joint (over time) posterior distribution by fitting the model's trajectory to available observations by adjusting a well-chosen set of control parameters (Dimet and Talagrand 1986), and

sequential methods that follow a probabilistic framework in which the estimation problem is split into successive cycles of alternating forecast and analysis steps (Künsch 2001). The forecast step computes the forecast probability density function (pdf) of the current state given past observations, by integrating the previous analysis pdf with the model. The forecast pdf is then updated in the analysis step with the incoming observation to obtain the analysis pdf of the state given all observations up to the current time. The analysis (ditto for the forecast) pdf contains all information about the state given the data, providing any type of state estimates as for instance the posterior mean (PM), which minimizes the mean-squared error (MSE) (van Trees 1968).

In practice, however, analytic calculation of these distributions is usually not possible unless the state-space system is linear and Gaussian, in which case the aforementioned filtering process reduces to the Kalman filter (KF) (Kalman 1960; Jazwinski 1970). The particle filter (PF) is the most prominent among the vast toolbox of numerical filtering methods that have been proposed for nonlinear/non-Gaussian systems (Gordon *et al.* 1993; Doucet *et al.* 2001). It is a Monte Carlo (MC) algorithm that provides a discrete approximation of the forecast and analysis distributions by random samples, called particles. The theory behind PF is mathematically sound and asymptotic (in the number of particles) convergence properties are well established (Doucet *et al.* 2001; Crisan and Doucet 2002). However, due to the finite number of particles that can be used in practice, the particles' weights usually exhibit variance that exponentially increases with time, often causing the filter divergence. This is known as the weights' degeneracy phenomenon in which all but a few particles will have negligible weights after few assimilation cycles only (Liu and Chen 1998; Doucet *et al.* 2001). This happens in part because the incoming observations are not used to update the particles in the analysis step, but only their weights (Hoteit *et al.* 2008; van Leeuwen 2009; Hoteit *et al.* 2012). A standard solution to mitigate the degeneracy phenomenon is resampling, which basically draws "new" particles by duplicating those with large weights and abandoning those with low weights (Rubin 1988; Gordon *et al.* 1993). The PF with resampling has been proven to perform well with low-dimensional systems (Kivman 2003), but its application to large-dimensional systems is still harmed by the required prohibitive number of particles to properly sample the state-space (curse of dimensionality) (Crisan and Doucet 2002; Snyder *et al.* 2008).

The ensemble KF (EnKF) is an MC implementation of the KF designed for large-dimensional systems. It uses the same forecast step as the PF, and an analysis step that is derived from that of the KF based on the Gaussian assumption on the joint state-observation forecast pdf. In the EnKF analysis step, the analysis particles (called "analysis members") can be sampled either by directly updating the forecast members with the KF correction step based on stochastically perturbed observations (Burgers *et al.* 1998; Houtekamer and Mitchell 1998; Evensen 2006), or through an update of the mean and a square-root form of the covariance of the forecast ensemble exactly as in the KF, without perturbing the observations (e.g. Bishop *et al.* 2001; Anderson 2001; Tippett *et al.* 2003; Hoteit *et al.* 2015). The KF correction pulls the ensemble members towards the observations, which should help mitigating the risk of degeneracy (Kivman 2003; Hoteit *et al.* 2008). In practice, the EnKF may suffer from undesirable effects originating from systematic and sampling errors (Whitaker *et al.* 2008; Houtekamer and Mitchell 2005). Systematic errors are due to* (i) uncertainties in the (parameters and dynamics) of the system under study, and misspecification of the state and observation noise models, and (ii) approximations in the filter, which are typically caused by the linear KF-like update, a consequence of the Gaussian assumption of its KF-update step. Sampling errors are due to the implementation of the EnKF with small ensembles to avoid excessive computational cost. If these deficiencies are not taken into account, the covariance of the forecast ensemble will suffer from (a) a deficient error covariance rank, (b) an underestimated (diagonal) variance, and (c) overestimated (off-diagonal) cross-covariance terms (Furrer and Bengtsson 2007; Whitaker and Hamill 2002). This may result in poor filter performances and sometimes even divergence; the so-called inbreeding problem (Furrer and Bengtsson 2007).

Even though systematic errors in the system and model noises (issue (i)) may be partially treated using well-known parameters estimation techniques (e.g. Dee 2005; Gharamti *et al.* 2015;

*Let notice that issues (i) are specific to any data assimilation method.

Ait-El-Fquih *et al.* 2016; Dreano *et al.* 2017; Sakov *et al.* 2018; Ait-El-Fquih and Hoteit 2018), and those in the filter (issue (ii)) by for instance relaxing the Gaussian assumption made on the analysis pdf to a Gaussian-mixture through the use of an ensemble Gaussian mixture filter (e.g. Hoteit *et al.* 2008, 2012; Frei and Künsch 2013; Liu *et al.* 2015), sampling errors are inevitable. Many applications have demonstrated that the EnKF can tolerate sampling errors by applying auxiliary techniques, the most standard of which are covariance inflation (Anderson 2001) and covariance localization (Houtekamer and Mitchell 1998) (other techniques have been also proposed, e.g. Hamill and Snyder (2000); Song *et al.* (2010); Luo and Hoteit (2011)). Localization tackles the problems of rank deficiency and underestimation of cross-covariances (issues (a)-(b)), by suppressing spurious correlations between distant state variables. Inflation counteracts the problem of underestimation of forecast variance (issue (c)) by artificially increasing the ensemble spread, either by a multiplicative factor (e.g. Anderson and Anderson 1999; Anderson 2007a; Miyoshi 2011; Kotsuki *et al.* 2017), or an additive factor (e.g. Mitchell and Houtekamer 2000; Whitaker and Hamill 2012), among others.

EnKF performances can be sensitive to the choice of inflation and localization scales, which require judicious tuning to achieve satisfactory results. Trial and error tuning of the parameters of these techniques can be computationally very demanding (Houtekamer and Mitchell 1998; Miyoshi 2011). Developing adaptive methods for online estimation of the localization length scale (e.g. Anderson 2007b; Bishop and Hodyss 2009a,b; Smidl and Hofman 2011) and the inflation factor (e.g. Anderson 2007a; Miyoshi 2011; Whitaker and Hamill 2012) is therefore of great interest. Here, we investigate the adaptive multiplicative inflation problem which received wide attention in recent years. This lead to the development of various methods that could be split into (i) trace-based methods, which basically match innovation covariances (Wang and Bishop 2003; Li *et al.* 2009), (ii) maximum likelihood (ML) methods, which aim at maximizing the likelihood of the inflation factor (Mitchell and Houtekamer 2000; Zheng 2009; Liang *et al.* 2012), and (iii) Bayesian methods, which exploit not only the observations, but also prior information about the inflation factor through a prior pdf (Anderson 2007a; Li *et al.* 2009; Brankart *et al.* 2010; Smidl and Hofman 2011; Miyoshi 2011; Raanes *et al.* 2018). Compared to the ML and trace-based approaches, the Bayesian approach suggests a more general and unifying framework that is not restricted to Gaussian errors and provides not only point estimates of the inflation factor, but more generally its (full) posterior distribution.

Adaptive inflation Bayesian methods generally differ in the choice of the prior pdf, the computation of the likelihood and/or the posterior, or in the underlying assumptions. In this work, we propose a new adaptive inflation algorithm combining the EnKF to estimate the state and the PF to estimate the inflation factor. The remainder of the paper is organized as follows. Section 2 states the problem and reviews the EnKF. Section 3 derives the proposed adaptive PF-type inflation scheme, and discusses the main differences with existing algorithms. Section 4 presents the results of numerical experiments with the Lorenz-96 model, and Section 5 concludes the work and discusses future directions.

2. Ensemble Kalman filter

2.1. *Bayesian filtering*

The problem consists of estimating an unknown (state) process, $\mathbf{x} = \{\mathbf{x}_n\}_{n\in\mathbb{N}}$, from an observed process, $\mathbf{y} = \{\mathbf{y}_n\}_{n\in\mathbb{N}}$, with $\mathbf{x}_n \in \mathbb{R}^{n_\mathbf{x}}$ and $\mathbf{y}_n \in \mathbb{R}^{n_\mathbf{y}}$ denoting the system state and the observation at time t_n, respectively. These are generally governed by a state-space system of the form

$$\left\{\begin{array}{rcl} \mathbf{x}_n &=& \mathbf{f}_{n-1}\left(\mathbf{x}_{n-1}\right) + \mathbf{u}_{n-1}, \\ \mathbf{y}_n &=& \mathbf{h}_n(\mathbf{x}_n) + \mathbf{v}_n, \end{array}\right. \tag{1}$$

where $\mathbf{f}_{n-1}(.)$ is a dynamical operator integrating the state from time t_{n-1} to t_n, and $\mathbf{h}_n(.)$ an observational operator at time t_n. As is often the case, the state dimension, $n_\mathbf{x}$, is assumed to be larger than the observation dimension, $n_\mathbf{y}$. The state noise process, $\mathbf{u} = \{\mathbf{u}_n\}_{n\in\mathbb{N}}$, and the observation noise process, $\mathbf{v} = \{\mathbf{v}_n\}_{n\in\mathbb{N}}$, are assumed to be independent, jointly independent and independent of the initial state, $\mathbf{x}_0$. Let also $\mathbf{u}_n$ and $\mathbf{v}_n$ be Gaussian with zero means and covariances, $\mathbf{Q}_n$ and $\mathbf{R}_n$, respectively. Throughout the paper, $p(\boldsymbol{\xi})$ and $p(\boldsymbol{\xi}|\boldsymbol{\mu})$ denote the pdf of a random variable, $\boldsymbol{\xi}$, and the conditional pdf of $\boldsymbol{\xi}$ given a realization of another random variable, $\boldsymbol{\mu}$, respectively. The independence properties of $\mathbf{u}$, $\mathbf{v}$ and

$\mathbf{x}_0$ yield,

$$p(\mathbf{x}_n|\mathbf{x}_{0:n-1},\mathbf{y}_{0:n-1}) = p(\mathbf{x}_n|\mathbf{x}_{n-1}), \quad (2)$$

$$p(\mathbf{y}_n|\mathbf{x}_{0:n},\mathbf{y}_{0:n-1}) = p(\mathbf{y}_n|\mathbf{x}_n), \quad (3)$$

which entails that the system (1) is a particular hidden Markov chain (HMC) of transition density, $p(\mathbf{x}_n|\mathbf{x}_{n-1})$, and likelihood, $p(\mathbf{y}_n|\mathbf{x}_n)$, of the form (e.g. Ait-El-Fquih and Desbouvries 2006) :

$$p(\mathbf{x}_n|\mathbf{x}_{n-1}) = \mathcal{N}_{\mathbf{x}_n}(\mathbf{f}_{n-1}(\mathbf{x}_{n-1}),\mathbf{Q}_{n-1}), \quad (4)$$

$$p(\mathbf{y}_n|\mathbf{x}_n) = \mathcal{N}_{\mathbf{y}_n}(\mathbf{h}_n(\mathbf{x}_n),\mathbf{R}_n), \quad (5)$$

where $\mathcal{N}_{\mathbf{x}}(\mathbf{m},\mathbf{C})$ stand for a Gaussian pdf of argument $\mathbf{x}$ and parameters $(\mathbf{m},\mathbf{C})$.

Bayesian filtering refers to the (online) estimation of the state, $\mathbf{x}_n$, given the set of observations, $\mathbf{y}_{0:n}=\{\mathbf{y}_0,\cdots,\mathbf{y}_n\}$, and involves the computation of the posterior pdf, $p(\mathbf{x}_n|\mathbf{y}_{0:n})$, known as filtering or analysis pdf. Any estimate of $\mathbf{x}_n$ from $\mathbf{y}_{0:n}$ can be deduced from this density depending on the choice of the optimization criteria. Here, we focus on the PM estimate, and the associated error covariance as a "measure" of estimate uncertainty.

Thanks to independence properties (2)-(3), it is possible to update the analysis pdf in a recursive way (Künsch 2001). This can be achieved with a succession of a Markovian step where the transition pdf, $p(\mathbf{x}_n|\mathbf{x}_{n-1})$, is used to obtain the forecast pdf,

$$p(\mathbf{x}_n|\mathbf{y}_{0:n-1}) = \int p(\mathbf{x}_n|\mathbf{x}_{n-1})p(\mathbf{x}_{n-1}|\mathbf{y}_{0:n-1})d\mathbf{x}_{n-1}, \quad (6)$$

and a Bayesian step in which the likelihood, $p(\mathbf{y}_n|\mathbf{x}_n)$, is combined with the forecast pdf using Bayes' rule,

$$p(\mathbf{x}_n|\mathbf{y}_{0:n}) \propto p(\mathbf{y}_n|\mathbf{x}_n)p(\mathbf{x}_n|\mathbf{y}_{0:n-1}). \quad (7)$$

In practice, analytical calculation of pdfs (6)-(7) and their first two moments is generally not feasible. The EnKF has been introduced as an efficient approach to provide MC approximations of these quantities, especially when it comes to large-dimensional systems.

2.2. *Ensemble Kalman filter (EnKF)*

The EnKF is an MC Gaussian-like implementation of the generic algorithm (6)-(7). Here, we follow its stochastic formulation, but the proposed adaptive inflation algorithm is still directly applicable to any other (deterministic) EnKF-type scheme (e.g. Anderson 2001; Tippett *et al.* 2003; Hoteit *et al.* 2015). Let for any ensemble $\{\boldsymbol{\xi}^m\}_{m=1}^M$, $\hat{\boldsymbol{\xi}}$ and $\mathbf{P}_{\boldsymbol{\xi}}$ denote its empirical mean and covariance, respectively; and $\mathbf{P}_{\boldsymbol{\xi},\boldsymbol{\mu}}$ the cross-covariance between $\{\boldsymbol{\xi}^m\}_{m=1}^M$ and $\{\boldsymbol{\mu}^m\}_{m=1}^M$. Starting from an ensemble of M (analysis) members, $\{\mathbf{x}_{n-1}^{a,m}\}_{m=1}^M$, sampled from $p(\mathbf{x}_{n-1}|\mathbf{y}_{0:n-1})$, the EnKF forecast samples a (forecast) ensemble, $\{\mathbf{x}_n^{f,m}\}_{m=1}^M$, from $p(\mathbf{x}_n|\mathbf{y}_{0:n-1})$ by integrating the analysis members forward with the model as,

$$\mathbf{x}_n^{f,m} = \mathbf{f}_{n-1}(\mathbf{x}_{n-1}^{a,m}) + \mathbf{u}_{n-1}^m, \quad (8)$$

with $\mathbf{u}_{n-1}^m$ sampled from the Gaussian, $\mathcal{N}(\mathbf{0},\mathbf{Q}_{n-1})$. Once a new observation, $\mathbf{y}_n$, is available, the analysis step is applied under the Gaussian assumption on $p(\mathbf{x}_n,\mathbf{y}_n|\mathbf{y}_{0:n-1})$, correcting the forecast members with a KF update step:

$$\mathbf{x}_n^{a,m} = \mathbf{x}_n^{f,m} + \hat{\mathbf{K}}_n(\mathbf{y}_n - \mathbf{y}_n^{f,m}), \quad (9)$$

where $\mathbf{y}_n^{f,m} = \mathbf{z}_n^{f,m} + \mathbf{v}_n^m$ is an observation forecast member, with $\mathbf{z}_n^{f,m} = \mathbf{h}_n(\mathbf{x}_n^{f,m})$ and $\mathbf{v}_n^m \sim \mathcal{N}(\mathbf{0},\mathbf{R}_n)$. The matrix, $\hat{\mathbf{K}}_n$, represents an ensemble-based approximation of the Kalman gain,

$$\mathbf{K}_n = \mathrm{cov}[\mathbf{x}_n,\mathbf{y}_n|\mathbf{y}_{0:n-1}]\times\mathrm{cov}[\mathbf{y}_n|\mathbf{y}_{0:n-1}]^{-1}, \quad (10)$$

$$= \mathrm{cov}[\mathbf{x}_n,\mathbf{z}_n|\mathbf{y}_{0:n-1}]\times(\mathrm{cov}[\mathbf{z}_n|\mathbf{y}_{0:n-1}]+\mathrm{cov}[\mathbf{v}_n])^{-1}; \quad (11)$$

$\mathrm{cov}[\boldsymbol{\xi}]$ and $\mathrm{cov}[\boldsymbol{\xi},\boldsymbol{\mu}]$ respectively denote the covariance of $\boldsymbol{\xi}$ and the cross-covariance between $\boldsymbol{\xi}$ and $\boldsymbol{\mu}$. It is thus given by,

$$\hat{\mathbf{K}}_n = \mathbf{P}_{\mathbf{x}_n^f,\mathbf{y}_n^f}\mathbf{P}_{\mathbf{y}_n^f}^{-1}, \quad (12)$$

if (10) is used, or by,

$$\hat{\mathbf{K}}_n = \mathbf{P}_{\mathbf{x}_n^f,\mathbf{z}_n^f} \times \left(\mathbf{P}_{\mathbf{z}_n^f} + \mathbf{R}_n\right)^{-1}, \quad (13)$$

if (11) is used. The latter would be more suitable in practice due to its lower MC randomness, especially when it comes to small ensembles. This is because $\mathrm{cov}[\mathbf{x}_n, \mathbf{v}_n|\mathbf{y}_{0:n-1}]$ and $\mathrm{cov}[\mathbf{v}_n]$ are set in (13) to their exact values, $\mathbf{0}$ and $\mathbf{R}_n$, respectively, while (12) rather uses ensemble-based estimates of these quantities, which should be affected by errors.

The Gaussian assumption on $p(\mathbf{x}_n, \mathbf{y}_n|\mathbf{y}_{0:n-1})$ holds if and only if (i) the forecast pdf is Gaussian, (ii) the likelihood, $p(\mathbf{y}_n|\mathbf{x}_n)$, is Gaussian, and (iii) the mean of this likelihood is a linear function of $\mathbf{x}_n$. Relating this with the noises of the nonlinear system (1), a Gaussian $\mathbf{v}_n$ entails (ii) only, and a Gaussian $\mathbf{u}_n$ will only partially contribute to satisfy (i). To tackle the deficiencies due to the fact that (i) and (iii) are not fulfilled, among others (e.g., ensemble sampling errors, poorly known noise statistics), the covariance inflation became one of the most popular techniques.

3. PF-based adaptive inflation scheme

Multiplicative covariance inflation expands the forecast members away from the mean using a factor, $\lambda > 1$, as,

$$\tilde{\mathbf{x}}_n^{f,m} = \sqrt{\lambda}\mathbf{x}_n^{f,m} + (1 - \sqrt{\lambda})\hat{\mathbf{x}}_n^f, \tag{14}$$

so that the forecast spread increases by λ, i.e., the forecast covariance, $\mathbf{P}_{\mathbf{x}_n^f}$, is inflated as,

$$\widetilde{\mathbf{P}}_{\mathbf{x}_n^f} = \lambda \mathbf{P}_{\mathbf{x}_n^f}. \tag{15}$$

Indirectly inflating the background covariance using (14), or directly using (15), do not have the same impact on the analysis step. Although these lead to the same inflated covariance, hence the same Kalman gain, their associated analysis steps operate on different forecast ensembles. As emphasized in Frei (2013), if one is only concerned with sampling errors, then (15) is suitable as there is no reason to modify the forecast ensemble. In the more general case where systematic errors are also involved, (14) would be more suitable.

3.1. Marginal versus joint Bayesian approach

In a Bayesian setting, the inflation factor is considered as a random variable with a prior pdf, $p(\lambda)$. The most natural way to estimate it, along with the state, is to follow a joint estimation approach, which involves evaluating the joint pdf, $p(\mathbf{x}_n, \lambda|\mathbf{y}_{0:n})$. This can be achieved by computing $p(\lambda|\mathbf{y}_{0:n})$ and $p(\mathbf{x}_n|\lambda, \mathbf{y}_{0:n})$ separately then taking,

$$p(\mathbf{x}_n, \lambda|\mathbf{y}_{0:n}) = p(\mathbf{x}_n|\lambda, \mathbf{y}_{0:n})p(\lambda|\mathbf{y}_{0:n}). \tag{16}$$

The inflation factor acts on "the analysis pdf", $p(\mathbf{x}_n|\lambda, \mathbf{y}_{0:n})$, through "the forecast pdf", $p(\mathbf{x}_n|\lambda, \mathbf{y}_{0:n-1})$, using Bayes' rule :

$$p(\mathbf{x}_n|\lambda, \mathbf{y}_{0:n}) \propto p(\mathbf{y}_n|\mathbf{x}_n)p(\mathbf{x}_n|\lambda, \mathbf{y}_{0:n-1}). \tag{17}$$

Unlike the augmented approach, which concatenates $\mathbf{x}_n$ and λ in the same vector, the separate approach (16) makes it possible to assign $p(\mathbf{x}_n|\lambda, \mathbf{y}_{0:n})$ and $p(\lambda|\mathbf{y}_{0:n})$ different probability laws. This is of a practical interest as $p(\mathbf{x}_n|\lambda, \mathbf{y}_{0:n})$, which will be computed using EnKF, is (by assumption) Gaussian, whereas $p(\lambda|\mathbf{y}_{0:n})$ can be any distribution with positive support.

The computation of $p(\mathbf{x}_n, \lambda|\mathbf{y}_{0:n})$ via (16) can be done by drawing (analysis) inflation samples, $\lambda_n^{a,m}$, from $p(\lambda|\mathbf{y}_{0:n})$ and then using them to sample the (analysis) state members, $\mathbf{x}_n^{a,m}$, from $p(\mathbf{x}_n|\lambda_n^{a,m}, \mathbf{y}_{0:n})$. This hierarchical sampling procedure has been recently applied by Ait-El-Fquih and Hoteit (2018) in the context of a state-parameter estimation problem. However, unlike (14), which applies the same inflation factor to all state forecast members, this approach rather assigns a different inflation factor to each member, i.e.,

$$\tilde{\mathbf{x}}_n^{f,m} = \sqrt{\lambda_n^{a,m}}\mathbf{x}_n^{f,m} + (1 - \sqrt{\lambda_n^{a,m}})\hat{\mathbf{x}}_n^f; \quad m = 1, \cdots, M. \tag{18}$$

The problem with (18) is that it is actually not a covariance inflation procedure per se because the forecast mean is not conserved, and the forecast covariance is not (multiplicatively) inflated as in (15). Indeed, (18) results in an ensemble with a biased mean,

$$\widehat{\tilde{\mathbf{x}}}_n^f = \hat{\mathbf{x}}_n^f + \underbrace{\sum_{m=1}^{M} \sqrt{\lambda_n^{a,m}}(\mathbf{x}_n^{f,m} - \hat{\mathbf{x}}_n^f)/M}_{\text{bias}}. \tag{19}$$

One could circumvent these issues by directly using (15), but this would lead to an analysis step that uses a different Kalman gain for each member, which is computationally unsuitable. Furthermore, practical issues, most notably spurious correlations and discrete jumps between the ensemble localization subdomains, are likely to occur as reported in Raanes *et al.* (2018).

In that respect, existing methods basically treat the state and inflation distributions separately; the so-called "marginal" methods (Raanes *et al.* 2018). In this approach, the inflation filter feeds the state filter with a point estimate (e.g., PM or maximum *a posteriori*, MAP), instead of the whole ensemble, $\{\lambda_n^{a,m}\}_{m=1}^M$. The estimate, $\widehat{\lambda}_n^a$, is indeed used to inflate the state forecast ensemble as in (14); the inflated ensemble, in turn, is updated based on the observation, $\mathbf{y}_n$, using an EnKF update step, yielding an analysis ensemble that is a sample of $p(\mathbf{x}_n|\widehat{\lambda}_n^a, \mathbf{y}_{0:n})$. In the next section, we propose a new marginal adaptive ensemble scheme involving MC approximations of the posterior inflation distribution, and subsequently its moments, using a PF-like algorithm. The derivation of the proposed PF-EnKF scheme assumes that $p(\mathbf{x}_n, \mathbf{y}_n|\lambda_n, \mathbf{y}_{0:n-1})$ is Gaussian, a standard assumption in the context of EnKF. This, in particular, implies that the marginal, $p(\mathbf{y}_n|\lambda_n, \mathbf{y}_{0:n-1})$, which will be used to compute the particles' weights, is Gaussian.

3.2. PF-EnKF algorithm

For simplicity, we start by assuming the inflation model to be static, i.e., $\lambda_n = \lambda_{n-1} = \lambda$. This entails,

$$p(\lambda_n|\mathbf{y}_{0:n-1}) = p(\lambda_{n-1}|\mathbf{y}_{0:n-1}). \tag{20}$$

The analysis pdf, $p(\lambda_n|\mathbf{y}_{0:n})$, can then be recursively computed only using Bayes' rule,

$$p(\lambda_n|\mathbf{y}_{0:n}) \propto p(\mathbf{y}_n|\lambda_n, \mathbf{y}_{0:n-1}) p(\lambda_{n-1}|\mathbf{y}_{0:n-1}), \tag{21}$$

where the (unknown) inflation likelihood is given as,

$$p(\mathbf{y}_n|\lambda_n, \mathbf{y}_{0:n-1}) = \int p(\mathbf{y}_n|\mathbf{x}_n) p(\mathbf{x}_n|\lambda_n, \mathbf{y}_{0:n-1}) d\mathbf{x}_n. \tag{22}$$

As stated above, $p(\mathbf{y}_n|\lambda_n, \mathbf{y}_{0:n-1})$ is inherently assumed Gaussian. Its moments can be empirically estimated from its samples. The samples can be drawn by plugging into (22) the inflated state forecast ensemble (14) (which is actually a sample of $p(\mathbf{x}_n|\lambda_n, \mathbf{y}_{0:n-1})$), then applying the well-known hierarchical sampling technique (e.g. Robert 2007). One readily obtains,

$$p(\mathbf{y}_n|\lambda_n, \mathbf{y}_{0:n-1}) \approx \mathcal{N}_{\mathbf{y}_n}(\widehat{\mathbf{z}}_n^f, \lambda_n \mathbf{P}_{\mathbf{z}_n^f} + \mathbf{R}_n). \tag{23}$$

Since λ_n is scalar, the PF provides an efficient mean for practical implementation of the above generic algorithm. In light of eq. (20), no forecast operation is involved in the PF, and thereby the inflation forecast particles, $\{\lambda_n^{f,s}\}_{s=1}^S$, are equal to the previous inflation analysis particles (i.e., $\lambda_n^{f,s} = \lambda_{n-1}^{a,s}$). The PF analysis is an MC implementation of the Bayesian step (21), and involves a weighting step then a resampling step (based on the well-known Rubin's sampling importance resampling (SIR) technique (Rubin 1988)). The weighting stage assigns to each particle, $\lambda_n^{f,s}$, a (normalized) weight, w_n^s, which, based on (23), is given as[†],

$$\begin{aligned} w_n^s &\propto \mathcal{N}_{\mathbf{y}_n}(\widehat{\mathbf{z}}_n^f, \mathbf{L}_n^s), \\ &\propto \left(\det[\mathbf{L}_n^s]\right)^{-1/2} \mathrm{e}^{-\frac{1}{2}\|\mathbf{y}_n - \widehat{\mathbf{z}}_n^f\|^2_{(\mathbf{L}_n^s)^{-1}}}, \end{aligned} \tag{24}$$

where $\mathbf{L}_n^s = \lambda_n^{f,s} \mathbf{P}_{\mathbf{z}_n^f} + \mathbf{R}_n$ and $\|\mathbf{v}\|^2_{\mathbf{M}} = \mathbf{v}^T \mathbf{M} \mathbf{v}$. The resulting weighted particles, $\{\lambda_n^{f,s}, w_n^s\}_{s=1}^S$, which represent an MC approximation of the (current) posterior, $p(\lambda_n|\mathbf{y}_{0:n})$, provide a point estimate, $\widehat{\lambda}_n^a$, and associated error variance, r_n^a, of λ_n given $\mathbf{y}_{0:n}$. The resampling step samples according to $\{\lambda_n^{f,s}, w_n^s\}_{s=1}^S$ with replacement to obtain a posterior set of particles, $\{\lambda_n^{a,s}, 1/\widetilde{S}\}_{s=1}^{\widetilde{S}}$. These (analysis) particles are *asymptotically* (on S) independent and identically distributed (iid) from the true analysis pdf, $p(\lambda_n|\mathbf{y}_{0:n})$, regardless of their number, $\widetilde{S}$ (Cappé *et al.* 2005, pp. 295–297). However, the independence property no longer holds when the forecast ensembles are finite (i.e., when S takes finite values), a case in which $\{\lambda_n^{a,s}\}_{s=1}^{\widetilde{S}}$ are only identically distributed (id) according to a pdf that differs from $p(\lambda_n|\mathbf{y}_{0:n})$ (Lamberti *et al.* 2017, Prop. 1). Further details can

[†] Without abuse of notation, $\mathcal{N}_u(.,.)$ denotes here the value of the Gaussian density at point u.

be found in Lamberti *et al.* (2017), who introduced an alternative resampling procedure providing iid particles, even with a finite S. For simplicity and as commonly done, we set $\widetilde{S} = S$ hereafter.

The practical implementation of the PF might still be prone to an issue caused by the finite character of S; this will be addressed in the subsequent section. A more efficient computation of the particles' weights will be also proposed in the case when the number of observations, $n_{\mathbf{y}}$, is large compared to the ensemble size, M.

2.2.1. *Dealing with a finite number of particles*

Estimating a static parameter using a PF with finite numbers of particles is often prone to the sample attrition issue (West and Liu 2001; Frei and Künsch 2012). Indeed, since the PF analysis is only a discrete sampling, the lack of a forecast step in the PF results in a loss of particles' diversity, and eventually one ends up with identical particles. This might be mitigated by introducing some dynamics for the (inflation) parameter. A popular dynamical model has been introduced by West and Liu (2001) in non-constrained real parameters' scenarios (i.e., $\lambda_n \in \mathbb{R}$), the so-called smoothing-kernel model:

$$\lambda_n = g(\lambda_{n-1}) + \epsilon_n, \tag{25}$$

where $g(\lambda_{n-1}) = \kappa\lambda_{n-1} + (1-\kappa)\widehat{\lambda}^a_{n-1}$ and ϵ_n a Gaussian noise with parameters,

$$\begin{cases} \mathbb{E}[\epsilon_n] &= 0, \\ \mathrm{var}[\epsilon_n] &= (1-\kappa^2) r^a_{n-1}, \end{cases} \tag{26}$$

with $\kappa \in]0,1[$. This model describes all possible dynamics from λ_{n-1} to λ_n (given $\mathbf{y}_{0:n-1}$) through a Gaussian transition density,

$$p(\lambda_n|\lambda_{n-1}, \mathbf{y}_{0:n-1}) = \mathcal{N}_{\lambda_n}(g(\lambda_{n-1}), (1-\kappa^2) r^a_{n-1}), \tag{27}$$

based on which the forecast pdf is then computed from the previous analysis pdf as,

$$p(\lambda_n|\mathbf{y}_{0:n-1}) = \int p(\lambda_n|\lambda_{n-1}, \mathbf{y}_{0:n-1}) p(\lambda_{n-1}|\mathbf{y}_{0:n-1}) d\lambda_{n-1}. \tag{28}$$

Model (25) is a more general alternative to the classical random walk model ($\lambda_n = \lambda_{n-1} + \epsilon_n$; $\mathrm{var}[\epsilon_n] =$ constant), which is prone to a systematic increase (over time) in the forecast variance, leading to forecast particles that are far too diffuse (Frei and Künsch 2012). Parameters (26) mitigate the particles over-dispersion by shrinking the values of λ_n (given $\mathbf{y}_{0:n-1}$) towards the previous mean, $\widehat{\lambda}^a_{n-1}$, so that both means and variances are conserved (i.e., $\widehat{\lambda}^f_n = \widehat{\lambda}^a_{n-1}$ and $r^f_n = r^a_{n-1}$). These moments are conserved regardless of the value of the parameter, κ, representing the degree of shrinkage.

Adapting West and Liu (2001) model to our case requires imposing the positivity constraint; more exactly enforcing $\lambda_n \geq 1$ to model the inflation, or $\lambda_n \geq 0$ to also account for the possibility of "deflation", yet a less frequent scenario. We further slightly modify this model to avoid a systematic decrease in the inflation variance (Chui and Chen 1987; Anderson 2007a) by imposing $r^f_n = \theta r^a_{n-1}$, with $\theta \geq 1$. This issue can be addressed by choosing a value of θ larger than 1 if r^a_{n-1} is below a threshold, and equal to 1, otherwise. With this revised model, the noise moments (26) become,

$$\begin{cases} \mathbb{E}[\epsilon_n] &= 0, \\ \mathrm{var}[\epsilon_n] &= (\theta-\kappa^2) r^a_{n-1}. \end{cases} \tag{29}$$

A natural way to constrain λ_n to be larger than a threshold l (l here is 0 or 1) would be to truncate the Gaussian noise distribution originally considered by West and Liu (2001), at point $l - g(\lambda_{n-1})$. This, however, prevents any analytical expression for the parameters of the associated truncated Gaussian transition pdf, $p(\lambda_n|\lambda_{n-1}, \mathbf{y}_{0:n-1})$, that satisfy (29). We thus resort to an inverse-Gamma transition pdf, one of the densities whose parameters can be analytically calculated, while imposing condition (29) in the framework of the model (25). Let $p(\lambda_n|\lambda_{n-1}, \mathbf{y}_{0:n-1}) = IG(\alpha_n, \beta_n)$, an inverse-Gamma density with shape and scale parameters, α_n and β_n, respectively. These parameters can be obtained by equating the moments,

$$\begin{cases} \mathbb{E}[\lambda_n|\lambda_{n-1}, \mathbf{y}_{0:n-1}] &= g(\lambda_{n-1}), \\ \mathrm{var}[\lambda_n|\lambda_{n-1}, \mathbf{y}_{0:n-1}] &= (\theta-\kappa^2) r^a_{n-1}, \end{cases} \tag{30}$$

which are actually equivalent to those in (29) regardless of the nature of $p(\epsilon)$, with the mean $\beta_n/(\alpha_n - 1)$ and the variance

$\beta_n^2/(\alpha_n-1)^2(\alpha_n-2)$ of $IG(\alpha_n,\beta_n)$. One readily obtains,

$$\begin{cases} \alpha_n &= \frac{g(\lambda_{n-1})^2}{(\theta-\kappa^2)r_{n-1}^a}+2, \\ \beta_n &= (\alpha_n-1)g(\lambda_{n-1}). \end{cases} \quad (31)$$

This results in a forecast step that samples the forecast particles, $\lambda_n^{f,s}$, from $IG(\alpha_n^s,\beta_n^s)$, where α_n^s and β_n^s correspond to $\lambda_{n-1}=\lambda_{n-1}^{a,s}$ in (31).

The inverse-Gamma choice includes the possibility of deflation due to its $\mathbb{R}^+$ support. If one wishes to ignore this possibility, the uniform density could be used due to its flexibility in choosing boundaries of the prior interval (a model with uniform noise is proposed in the appendix). In the numerical experiments conducted in this study, we use only the inverse-Gamma case which, based on several tests, was revealed to overally exhibit a slightly better behavior.

3.2.2. *Dealing with a large number of observations*

Computing w_n^s using (24) involves the inverse and determinant of the $n_{\mathbf{y}}\times n_{\mathbf{y}}$ matrix, $\mathbf{L}_n^s$. Inverting the expression $\lambda_n^{f,s}\mathbf{P}_{\mathbf{z}_n^f}+\mathbf{R}_n$ of $\mathbf{L}_n^s$, or calculating its determinant, leads to a cubic computational cost, in $n_{\mathbf{y}}$. Treating the problem in the ensembles space, this cubic cost can be reduced if $n_{\mathbf{y}}$ is larger than M (or more precisely reduced to a linear cost if $n_{\mathbf{y}}$ is quite larger than M), when $\mathbf{R}_n$ is diagonal, a classical assumption in geophysical applications, or block-diagonal with small blocks. This can be achieved by instead computing the determinant and the inverse of the smaller $M\times M$ matrix, $\mathbf{\Delta}_n^s=(\lambda_n^{f,s})^{-1}\mathbb{I}_M+\mathbf{S}_{\mathbf{z}_n^f}^T\mathbf{\Gamma}_n\mathbf{S}_{\mathbf{z}_n^f}$, with $\mathbf{S}_{\mathbf{z}_n^f}$ being the $n_{\mathbf{y}}\times M$ perturbation matrix of $\mathbf{P}_{\mathbf{z}_n^f}$ (i.e., $\mathbf{P}_{\mathbf{z}_n^f}=\mathbf{S}_{\mathbf{z}_n^f}\mathbf{S}_{\mathbf{z}_n^f}^T$) and $\mathbf{\Gamma}_n=\mathbf{R}_n^{-1}$, then using,

$$\left(\mathbf{L}_n^s\right)^{-1} = \mathbf{\Gamma}_n-\mathbf{\Gamma}_n\mathbf{S}_{\mathbf{z}_n^f}\times\left(\mathbf{\Delta}_n^s\right)^{-1}\times\mathbf{S}_{\mathbf{z}_n^f}^T\mathbf{\Gamma}_n, \quad (32)$$

$$\det\left[\mathbf{L}_n^s\right] = (\lambda_n^{f,s})^M\det[\mathbf{R}_n]\det\left[\mathbf{\Delta}_n^s\right]. \quad (33)$$

Eqs. (32) and (33) are derived using the well-known Woodbury matrix inversion lemma and the Sylvester's determinant theorem, respectively.

It turns out that for a narrow likelihood $p(\mathbf{y}_n|\lambda_n,\mathbf{y}_{0:n-1})$ (i.e., that peaks in a very small part of the observations space), the curse of dimensionality may still arise even when the space of parameters is small (which is our case as $\lambda_n\in\mathbb{R}$), unless the particles size, S, is substantially increased. As discussed in Bengtsson *et al.* (2008) (see also Snyder *et al.* 2008; van Leeuwen 2009), this scenario occurs particularly when the data involve a large number, $n_{\mathbf{y}}$, of conditionally independent and Gaussian observations. This suggests that $n_{\mathbf{y}}$ must be enough smaller than S to avoid the degeneracy of the weights (whether using the form (24) or (32)-(33)). Accordingly, eqs. (32)-(33) could be useful when $n_{\mathbf{y}}$ is larger than the ensemble size, M, but also smaller than S in such a way that the weights' degeneracy could be avoided.

3.2.3. *The PF-EnKF algorithm*

Once at time, t_n, the state forecast ensemble, $\{\mathbf{x}_n^{f,m}\}_{m=1}^M$, is computed in the EnKF forecast step (8), the PF is integrated to estimate the inflation value as follows:

- Forecast step. Given an (inflation) analysis ensemble, $\{\lambda_{n-1}^{a,s}\}_{s=1}^S$, use (31) with $\lambda_{n-1}=\lambda_{n-1}^{a,s}$ to compute α_n^s and β_n^s, then draw the forecast particles, $\lambda_n^{f,s}$, from $IG(\alpha_n^s,\beta_n^s)$.
- Analysis step. Compute the normalized weights, $\{w_n^s\}_{s=1}^S$, using (24), then an estimate, $\widehat{\lambda}_n^a$, and corresponding error variance, r_n^a, based on the weighted ensemble, $\{\lambda_n^{f,s},w_n^s\}_{s=1}^S$. In the case $n_{\mathbf{y}}\gg M$, use (32)-(33) in (24) if $\mathbf{R}_n$ is (block) diagonal to efficiently compute the weights. Finally, sample $\{\lambda_n^{f,s},w_n^s\}_{s=1}^S$ to obtain an equi-weighted analysis ensemble, $\{\lambda_n^{a,s},1/S\}_{s=1}^S$.

The estimate, $\widehat{\lambda}_n^a$, is then used to inflate the state forecast ensemble as in (14). The inflated ensemble is then updated in the EnKF analysis as in ((9),(13)), which results in an analysis ensemble, $\{\mathbf{x}_n^{a,m}\}_{m=1}^M$. The PF could be initialized (at $n=0$) using any distribution of positive support. For instance, if one wants to draw the particles such that their empirical mean and variance respectively match given values, $\overline{\lambda}$ and $\overline{r}$ (i.e., to constrain $\widehat{\lambda}_0^f$ and r_0^f to be - approximately - equal to $\overline{\lambda}$ and $\overline{r}$, respectively), one could sample from the uniform law, $\mathcal{U}[\overline{\lambda}-\sqrt{3\overline{r}},\overline{\lambda}+\sqrt{3\overline{r}}]$, or from the inverse-Gamma law, $IG(\alpha,\overline{\lambda}(\alpha-1))$, with $\alpha=2+\overline{\lambda}^2/\overline{r}$. As stated above, parameter θ (which arises along with κ in the computation of the weights) can be chosen as equal to 1 if r_{n-1}^a is below a threshold, and larger than 1 otherwise.

As for the shrinkage parameter, κ, a theoretical "optimal" value could be calculated similarly to West and Liu (2001) (see eq. (23)), by assuming $p(\epsilon_n)$ to be an inverse-Gamma instead of a Gaussian pdf. This is left for a future work. In practice, and as is well-known, the empirical choice of κ is not too critical. In our numerical experiments, κ was set to 0.9, but larger values have provided comparable results.

The proposed PF-EnKF is suitable for applications with large-dimensional state models. Indeed, since the state is estimated by the EnKF component in the proposed algorithm, increasing its dimension, $n_{\mathbf{x}}$, may in some situations require an increase of the ensemble size, M, as for any other EnKF-based assimilation system. On the other hand, the PF does not operate on the state (i.e., it does not involve $n_{\mathbf{x}}$) but rather on the sample mean, $\widehat{\mathbf{z}}_n^f$, and covariance, $\mathbf{P}_{\mathbf{z}_n^f}$, of the $n_{\mathbf{y}} \times 1$ members $\{\mathbf{z}_n^{f,m} = \mathbf{h}_n(\mathbf{x}_n^{f,m})\}_{m=1}^M$ (through the weights w_n^s). Therefore, one intuitively expects that for a fixed $n_{\mathbf{y}}$, if good performances are achieved by the PF for a given value of $n_{\mathbf{x}}$, M and S, then for any larger state size $\widetilde{n}_{\mathbf{x}}$, if $\widehat{\mathbf{z}}_n^f$ and $\mathbf{P}_{\mathbf{z}_n^f}$ are well estimated using a (possibly larger) ensemble size $\widetilde{M}$, the PF should still provide good performances without increasing S.

3.2.4. *Discussion*

The proposed approach treats the inflation factor and the system state in a marginal way (separately) for online estimation of their posterior distributions within a Bayesian framework. Conceptually, at each assimilation cycle, the inflation factor is first estimated using a PF, then used in the EnKF to enhance the state estimation by inflating the underlying forecast ensemble. While the joint approach is based on a fully Bayesian factorization of the joint analysis pdf of interest (i.e., eq. (16)), the marginal approach can be seen as an optimization technique approximating this density by the separable product,

$$p(\mathbf{x}_n, \lambda_n | \mathbf{y}_{0:n}) \approx p(\mathbf{x}_n | \widehat{\lambda}_n^a, \mathbf{y}_{0:n}) \delta(\lambda_n - \widehat{\lambda}_n^a), \qquad (34)$$

under the Kullback-Leibler minimization criteria, the so-called certainty equivalence principle (Smidl and Quinn 2008). Indeed, the proposed marginal approach involves two discrete MC approximations (of $\delta(\lambda_n - \widehat{\lambda}_n^a)$ and $p(\mathbf{x}_n | \widehat{\lambda}_n^a, \mathbf{y}_{0:n})$ using PF and EnKF, respectively) on top of the continuous functional approximation (34). Despite this, this approach remains more suitable in practice than the joint one, which requires computing one Kalman gain for each member in the EnKF update step, and imposes the same number of particles in the PF and EnKF.

To counteract the sample impoverishment issue which inevitably occurs in free-forecast PFs, the proposed PF employs a dynamical model for the inflation factor following the West and Liu (2001) approach. Such a model aims at sampling a forecast ensemble, not only by matching the mean and (approximately) the variance, a key principle of West and Liu (2001) to avoid sample over-dispersion over the time, but also by constraining the sampled particles to be positive, using an inverse-Gamma transition pdf whose parameters are explicitly calculated under the aforementioned moments' matching condition. This constitutes a major difference with Smidl and Hofman (2011), who instead considered a random walk model[‡] with truncated-Gaussian noise, which, as outlined above, is likely to meet the forecast over-dispersion issue.

Both forecast and analysis inflation pdfs are approximated in Anderson (2007a) by Gaussians, which allows negative and nonsensical values of inflation. Fitting the "true posterior" with a Gaussian enabled the author to compute the MAP and corresponding error variance, by solving a cubic equation. This was done by processing the observations serially subject to a diagonal $\mathbf{R}_n$. Such an approach was then extended to the spatio-temporal case where the state components are inflated with different inflation factors, first in Anderson (2009), then by Gharamti (2018) who proposed a modified likelihood as an attempt to reduce the possibility of deflation, and an inverse-Gamma prior to preclude negative inflation values. While the resulting posterior does not suggest any standard form, Gharamti (2018) assumed it inverse-Gamma and approximated its shape and scale parameters following a similar strategy to Anderson (2009). In the proposed PF, no assumption was made on the posterior distribution of the inflation factor. Instead, an inverse-Gamma assumption was made on the transition pdf, which does

[‡]Smidl and Hofman (2011) focused also on the online estimation of the localization scale and the observation noise variance. Our scheme can straightforwardly address this problem by concatenating in the same vector the tuning parameters of interest.

not necessarily lead to an analysis (or forecast) pdf that is inverse-Gamma, nor of any other particular form.

Another approach was proposed by Li *et al.* (2009), in which both prior (forecast) and likelihood pdfs of the inflation factor are inherently assumed to be Gaussian. Concretely, once an ML estimate is computed using the innovation statistics of Desroziers *et al.* (2005), this is then taken as the mean of the likelihood, based on which the KF analysis can be applied to compute a PM estimate of the inflation factor. A more explicit Bayesian interpretation of this approach has then been given by Miyoshi (2011), who further proposed an estimate of the posterior variance based on the central limit theorem. Miyoshi (2011)'s algorithm has been recently revisited by Raanes *et al.* (2018) in the context of the EnKF-N (Bocquet *et al.* 2015). The revised scheme imposes the positivity on the inflation factor by considering a χ^{-2} prior instead of a Gaussian. Another advantage of such a prior is that it allows to exploit the conjugacy property, which leads to a posterior that belongs to the same distributional family (i.e., χ^{-2}), further with parameters that can be analytically calculated given the likelihood. However, this requires assuming $\mathbf{P}_{\mathbf{z}_n^f}\mathbf{R}_n^{-1}$ to be a multiple of the identity matrix to be able to approximate the likelihood with a χ^{-2} density, in addition to other assumptions that were made on the parameters of the resulting likelihood to insure the conjugacy with the χ^{-2} prior.

4 Numerical experiments

Numerical experiments are performed with the strongly nonlinear Lorenz-96 (L96) model (Lorenz and Emanuel 1998) to assess the behavior of the proposed PF-EnKF and to evaluate its performances against the benchmark Anderson (2007a) algorithm (hereafter called A07). L96 describes the time evolution of an atmospheric quantity, solving the following set of differential equations:

$$\frac{dx(j,t)}{dt} = x(j-1,t)[x(j+1,t) - x(j-2,t)] - x(j,t) + F, \tag{35}$$

where $F = 8$ denotes the external forcing constant, and $x(j,t)$, $j = 1, \cdots, n_{\mathbf{x}} = 40$, the j^{th} element of the state at time t. Boundary conditions are cyclic, satisfying $x(-1,t) = x(n_{\mathbf{x}} - 1, t)$, $x(0,t) = x(n_{\mathbf{x}}, t)$, and $x(1,t) = x(n_{\mathbf{x}} + 1, t)$. We consider for now the standard case of a perfect model.

We use the fourth-order Runge-Kutta discretization scheme to numerically integrate the model (35) with a time step size $\delta_m = 0.05$, equivalent to six hours in real time. The reference (true) state trajectory is built with F as an initial state, and is used to evaluate the filters' performances. The model is then integrated for 37300 time steps (corresponding to 25.5479 years in real time). The first 30000 time steps of the resulting trajectory are discarded as a spin-up period, and the remaining 7300 time steps (i.e., five years) are considered as the reference states. The observations are obtained by adding to the odd-indexed elements of the reference state (i.e., $n_{\mathbf{y}} = 20$) a Gaussian noise with zero mean and covariance, $\mathbf{R}_n = \mathbb{I}_{n_{\mathbf{y}}}$.

In the PF component of the proposed scheme, we use in the model (29), $\kappa = 0.9$ and $\theta = 1.2$ if $r_{n-1}^a < 10^{-4}$, and $\theta = 1$ otherwise. These values are based on trial and error experiments. In both filters, the initial state ensemble is generated from a Gaussian density centered around the mean of the reference states with an identity covariance (Hamill and Whitaker 2010). Regarding the initialization of the inflation, the initial particles are sampled in the PF from a uniform density, $\mathcal{U}[1,2]$, while in A07 algorithm, which operates on the first two moments of the inflation pdfs, instead of their samples, we take 1.5 and 0.028 as initial mean and variance, respectively. This means that the two algorithms use the same initial mean (i.e., 1.5) and close spreads[§].

In all experiments, the PF is implemented with $S = 200$ particles, which suggests a roughly similar computational cost with the A07. A residual resampling is further performed in this filter whenever the effective number of particles, $S_{\text{eff}} = 1/w_n^2$ (Liu and Chen 1998), is below $0.8\,S$. The EnKF in both algorithms was implemented with covariance localization, using the fifth-order correlation function (Gaspari and Cohn 1999) with a localization length-scale $\ell = 2$.

We start by assessing the performances of the filters with $M = 20$ members in a setting where the data are assimilated every four model steps, which is equivalent to one day in real time (i.e., the observations' time step is $\delta_o = 4\delta_m$). The results

[§]This is because the variance, 0.028, of the prior that is used in A07 algorithm leads to a 99 % credible interval (CI), which almost coincides with the support of the prior, $\mathcal{U}[1,2]$, that is used in the proposed PF.

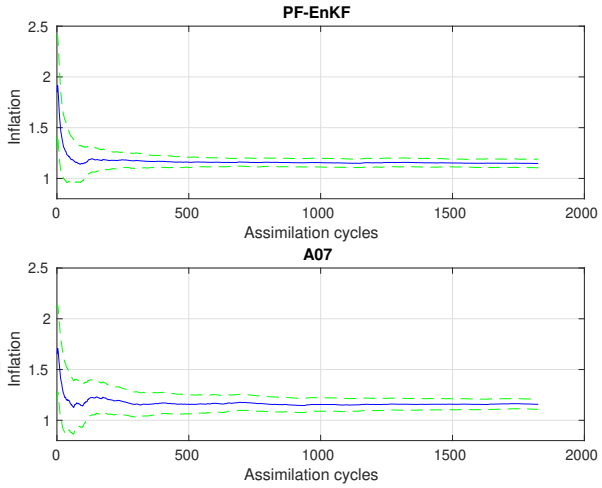

Figure 1. Time-evolution of the inflation analysis estimates (blue) and associated 99% credible intervals (dashed green) using the PF-EnKF and A07. In the EnKF component of both schemes the ensemble size and localization length scale were set to $M = 20$ and $\ell = 2$, respectively. The PF component of the proposed scheme was implemented with $S = 200$ particles. Observations were assimilated from half of the state variables at every four model time steps (one day in real time).

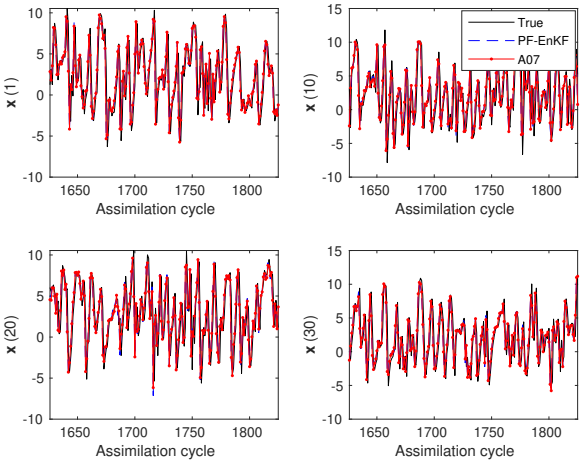

Figure 2. Time-evolution of the analysis estimates of the state elements, $\mathbf{x}(1)$, $\mathbf{x}(10)$, $\mathbf{x}(20)$ and $\mathbf{x}(30)$, as suggested by the PF-EnKF (dashed blue) and A07 (red); Black solid line represents the true state. In the EnKF component of both schemes the ensemble size and localization length scale were set to $M = 20$ and $\ell = 2$, respectively. The PF component of the proposed scheme was implemented with $S = 200$ particles. Observations were assimilated from half of the state variables at every four model time steps (one day in real time).

are averaged over 30 independent simulations, each time with a randomly generated initial ensembles and observation noise.

Figure 1 plots the time evolution of the inflation analysis estimates and associated 99% CIs. For both schemes, the inflation estimates mark a fast decrease in the early assimilation cycles, before they stabilize at about the 150-*th* assimilation cycle for the PF-EnKF and the 300-*th* for A07. This may reflect the large EnKF errors during the early period when only few observations are assimilated, before they reach their "optimal level" once enough observations have been incorporated. The PF-EnKF provides roughly similar estimates to the A07, with averaged inflation values over the latest 200 cycles are about 1.15 and 1.16 for PF-EnKF and A07, respectively, and slightly smaller CIs. Running the EnKF with the estimated inflation from both schemes leads to satisfactory state estimation, as shown in Figure 2, which displays the analysis estimates of some state elements. The MSE of the full state analysis estimate is further presented in Figure 3, suggesting a slightly better accuracy of the proposed PF-EnKF. Figure 4, which is a zoom of Figure 2, shows, in addition to the analysis estimates, the time averaged variance of these estimates (in the subtitles) along with the associated 99% CIs. Overall, while PF-EnKF suggests slightly smaller variances, both algorithms provide CIs that include the true states.

In the next set of experiments, we study the sensitivity of the two methods to different ensemble sizes and frequency of observations. We also perform the same study in two more

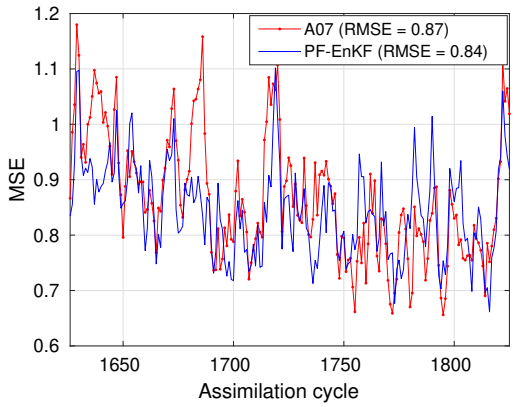

Figure 3. Time-evolution of the MSE of the analysis state estimate as suggested by the PF-EnKF (blue) and A07 (red); the averaged RMSE values are also given in the figure legend. In the EnKF component of both schemes the ensemble size and localization length scale were set to $M = 20$ and $\ell = 2$, respectively. The PF component of the proposed scheme was implemented with $S = 200$ particles. Observations were assimilated from half of the state variables at every four model time steps (one day in real time).

challenging scenarios, involving more pronounced systematic errors, one of which uses a perturbed state model in the two algorithms, and the other uses a perturbed observation model. In these experiments, the filters' performances are evaluated based on the root MSE (RMSE) misfits between the reference states and their filter analysis states, averaged over all variables and over the last 200 assimilation cycles (e.g. Raboudi *et al.* 2018, eq. (44)). For the inflation, we consider the analysis estimates and associated error variances averaged over the same temporal period. Temporal averages of these quantities turn out to be relevant indicators since, as will be seen, the estimates exhibit very low variability in time with very low variances. All the results are averaged over 30 independent repetitions.

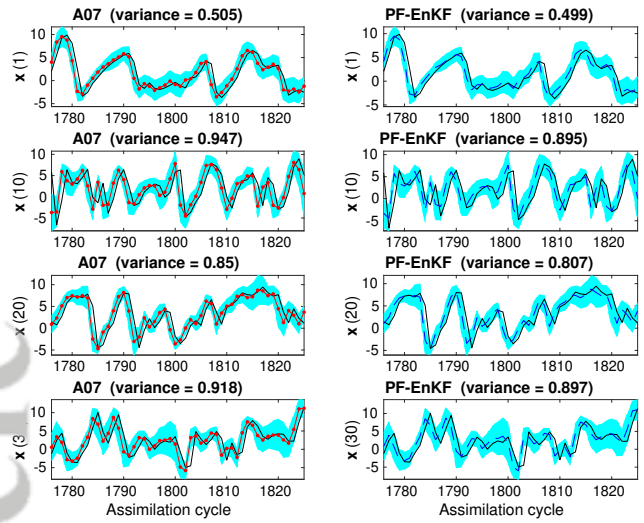

Figure 4. As in Fig. 2 (true states and their estimates using PF-EnKF and A07) on a reduced assimilation period, and 99% credible intervals (shaded cyan areas). The analysis variances averaged over the last 200 assimilation cycles are given in the subtitles.

4.1. Sensitivity study: the algorithms use the true models

We start by the sensitivity to the ensemble size, M. The other parameters are holding constant, in particular the data is assimilated every $\delta_o = 4\delta_m$. Table 1 displays, as a function of M, the time-averaged analysis inflation estimates, associated error variances, and variable- and time-averaged RMSE of the analysis state estimate. As can be seen, the inflation estimates and associated variances decrease with the ensemble size for both algorithms. The decrease is relatively pronounced between $M = 10$ and 20 members, and then progressively softens with larger ensembles (e.g., PF-EnKF provides inflation estimates whose average decreases of about 0.25 when moving from $M = 10$ to 20, and of 0.02 from $M = 40$ to 50). This may reflect the reduced sampling EnKF errors with larger ensembles. One may also notice that the (time-averaged) estimation error variances are very low ($\sim 10^{-4}$), which suggests that the values of both $\widehat{\lambda}_n^a$ and r_n^a are roughly constant in time; this is also true for all other experiments (see other tables). As for the state analysis RMSE, it decreases when increasing the ensemble size. Finally, the PF-EnKF exhibits a slightly better behavior than A07 for all values of M.

We now fix the ensemble size to $M = 20$ and use different lengths of assimilation windows, $f_0 = \delta_0/\delta_m$ (the times at which data are assimilated). As can be seen from Table 2, overall, the inflation factor estimated by both filters increases when the data is assimilated less frequently. This may reflect the increase of (systematic) errors in the EnKF when f_0 gets smaller, a situation in which larger values of $\widehat{\lambda}_n^a$ might be needed to mitigate for the loss of ensemble variance caused by these errors. As a matter of fact, the nonlinearity of the state model within the forecast period becomes more prominent for increased assimilation windows, which would make the Gaussianity assumption on which the EnKF is founded less reliable, thereby increasing the errors in the filter (i.e., the aforementioned systematic-type errors). As for the state analysis RMSE (rows c), it meets the expectations as it increases with f_0. Finally, once again, the PF-EnKF provides roughly smaller errors than A07.

4.2. Sensitivity study: the algorithms use a perturbed state model

Here, the reference states (and associated observations) are simulated, as above, with the perfect state-space model, whereas the two filtering algorithms use in their forecast steps an imperfect state model with additve Gaussian noise, $\mathbf{u}_n$, of zero mean and covariance, $\mathbf{Q}_n = 0.01\mathbb{I}$. This could be considered as some kind of additive inflation, therefore helps, along with the multiplicative inflation, mitigating for the sampling and systematic errors in the EnKF. Table 3 plots the results of the same experiments as those of Table 1, but conducted in the case of this perturbed state model. Similarly to the perfect model case, both filters provide inflation estimates and state estimation errors that decrease with the ensemble size. However, compared to the perfect model (Table 1), the noisy model (Table 3) leads for fixed values of M to smaller inflation estimates, but (mildly) larger state RMSEs. The decrease of the inflation estimates and increase (instead of decrease) of the resulting state RMSEs may be explained by the fact that these quantities involve different kinds of (state) errors. Structurally, the inflation acts on the error between the ensemble members and the PM estimate, $\mathbf{e}_1 = \mathbf{x}_n^{a,m} - \hat{\mathbf{x}}_n^a$, whereas the RMSE is based on the error between the true state and the PM estimate, $\mathbf{e}_2 = \mathbf{x}_n - \hat{\mathbf{x}}_n^a$. On the other hand, perturbing the state model with a $\mathcal{N}(\mathbf{0}, 0.01\mathbb{I})$ noise may be also seen as a new source of (systematic) errors, which would impose more errors in the filter compared to the perfect case. With that said, even though the smaller inflation values (in Table 3 compared to Table 1) may reflect smaller (averaged) errors $\mathbf{e}_1$, the resulting (more erroneous)

M	10	20	30	40	50
A07 (a)	1.397	1.161	1.102	1.069	1.0549
PF-EnKF (a)	1.397	1.149	1.087	1.072	1.054
A07 (b)	$3.47\ 10^{-4}$	$2.82\ 10^{-4}$	$2.67\ 10^{-4}$	$2.62\ 10^{-4}$	$2.58\ 10^{-4}$
PF-EnKF (b)	$3.51\ 10^{-4}$	$2.03\ 10^{-4}$	$1.97\ 10^{-4}$	$1.98\ 10^{-4}$	$2.18\ 10^{-4}$
A07 (c)	1.01	0.87	0.83	0.81	0.798
PF-EnKF (c)	0.98	0.84	0.81	0.79	0.78

Table 1. Estimation results as suggested by PF-EnKF and A07 as a function of ensemble size: Time-averaged estimate of the inflation parameter (rows (a)), associated error variance (rows (b)), and time- and variable-averaged RMSE of the state analysis estimates (rows (c)). In the EnKF component of both schemes, the localization length scale was set to 2, and in the PF component of the proposed scheme, the particles' number was set to 200. Observations were assimilated from half of the state variables at every four model time step (1 day in real time).

f_o	2	4	6	8	10
A07 (a)	1.079	1.161	1.186	1.1663	1.159
PF-EnKF (a)	1.094	1.149	1.1644	1.1484	1.1338
A07 (b)	$3.53\ 10^{-4}$	$2.82\ 10^{-4}$	$2.68\ 10^{-4}$	$2.77\ 10^{-4}$	$3.05\ 10^{-4}$
PF-EnKF (b)	$2.63\ 10^{-4}$	$2.03\ 10^{-4}$	$2.42\ 10^{-4}$	$2.23\ 10^{-4}$	$2.03\ 10^{-4}$
A07 (c)	0.574	0.87	1.23	1.663	2.0386
PF-EnKF (c)	0.5578	0.84	1.2186	1.6545	2.0153

Table 2. Estimation results as suggested by PF-EnKF and A07 as a function of the temporal assimilation period: Time-averaged estimate of the inflation parameter (rows (a)), associated error variance (rows (b)), and time- and variable-averaged RMSE of the state analysis estimates (rows (c)). In the EnKF component of both schemes, ensemble size and localization length scale were set to 20 and 2, respectively, and in the PF component of the proposed scheme, the particles' number was set to 200. Observations were assimilated from half of the state variables.

state estimates would be further away from the true state than those given in Table 1, which would lead to larger errors $\mathbf{e}_2$ and subsequently larger RMSEs. Finally, for this perturbed model also, the PF-EnKF suggests, overall, slightly smaller state RMSEs than A07.

We also ran the same experiments as those of Table 2 using this perturbed model; the results are displayed in Table 4. Once again, a similar behavior as the perfect case is observed, in particular, inflation estimates and state RMSEs increase with larger assimilation windows. Furthermore, for the same value of f_o, the inflation estimates slightly decrease when perturbing the model. As stated above, this suggests that this perturbation could be considered as an (additive) inflation. But at the same time, it is also an additional source of errors that induce more errors in the state estimates, which explains the larger RMSEs in Table 4.

Noticing that this perturbed state model scenario amounts to considering a state noise, $\mathbf{u}_n$, with a biased covariance, $\mathbf{Q}_n$, similar experiments have been also conducted for the case where the mean (instead of covariance) of $\mathbf{u}_n$ is biased. Due to the additive character of $\mathbf{u}_n$, introducing a bias in its mean amounts to assuming the state model to be biased. We used as a bias the one in Li *et al.* (2009), eq. (17), with $\alpha = 7$ (i.e., the case of the largest bias). Overall (results not shown to save space), PF-EnKF and, to a slightly lesser extent, A07, can account for state model bias most notably when large enough ensembles or not too large assimilation windows are used.

4.3. Sensitivity study: the algorithms use a perturbed observational model

Here, the two filtering algorithms use the perfect state model but a perturbed observation model in which the noise covariance is increased by 20% (i.e., $\mathbf{R}_n$ becomes $1.2\,\mathbf{R}_n$). In contrast with the case of perturbed state model, this should not be seen as an additional inflation in the EnKF, but only as an additional source of (systematic) errors in the filter. Table 5, which plots the results of the same experiments as those of Tables 1 and 3 but using this model, shows clearly larger state RMSEs for both schemes, which may be explained by the inclusion of more errors in the filter. On the other hand, with this perturbed observational model, the estimated inflation factor is significantly smaller than those obtained with the perfect and perturbed state models (see rows a of Tables 1, 3 and 5). Indeed, the perturbation of the observation noise would result in larger state analysis spreads, which, in turn, would lead to larger forecast spreads in the next assimilation cycle; for instance, some tests have shown that for PF-EnKF (resp. A07) with 20 members, the forecast spread is of about 0.97, 1.05

M	10	20	30	40	50
A07 (a)	1.3407	1.1004	1.0413	1.0089	0.9947
PF-EnKF (a)	1.3268	1.0911	1.0267	1.004	0.9933
A07 (b)	$3.02\ 10^{-4}$	$2.36\ 10^{-4}$	$2.24\ 10^{-4}$	$2.19\ 10^{-4}$	$2.16\ 10^{-4}$
PF-EnKF (b)	$4.25\ 10^{-4}$	$3.13\ 10^{-4}$	$3.19\ 10^{-4}$	$2.82\ 10^{-4}$	$2.69\ 10^{-4}$
A07 (c)	1.0522	0.8872	0.8353	0.8152	0.7987
PF-EnKF (c)	1.0255	0.8669	0.8327	0.8034	0.80105

Table 3. As in Tab. 1, but in the case of a perturbed state model.

f_o	2	4	6	8	10
A07 (a)	1.028	1.1004	1.1356	1.1333	1.1337
PF-EnKF (a)	1.029	1.0911	1.1186	1.1184	1.1115
A07 (b)	$2.8\ 10^{-4}$	$2.36\ 10^{-4}$	$2.42\ 10^{-4}$	$2.64\ 10^{-4}$	$2.92\ 10^{-4}$
PF-EnKF (b)	$3.04\ 10^{-4}$	$3.13\ 10^{-4}$	$3.31\ 10^{-4}$	$3.41\ 10^{-4}$	$3.27\ 10^{-4}$
A07 (c)	0.5869	0.8872	1.2531	1.6743	2.0421
PF-EnKF (c)	0.5833	0.8669	1.2373	1.6693	2.0158

Table 4. As in Tab. 2, but in the case of a perturbed state model.

and 1.95 (resp. 0.97, 1.05 and 1.91) in the true, perturbed state, and perturbed observational models, respectively. This automatic increase (inflation) of the forecast spread would explain the small values (overall, close to 1) of the inflation factor estimates.

Table 6 summarizes the results of the same experiments as those of Tables 2 and 4, but conducted with the perturbed observational model. Once again, similarly to the perfect and the perturbed state model cases, state RMSEs increase when less observations are assimilated. However, this is not generally true for the inflation estimates which instead slightly decrease with f_0. Finally, the proposed scheme suggests mildly more accurate state estimates for this noisier observation model as well.

5. Conclusion

We considered the problem of adaptive multiplicative covariance inflation in the context of the ensemble Kalman filter (EnKF). The problem was addressed within a Bayesian framework, where a prior probability distribution for the inflation factor is combined with the inflation likelihood through Bayes' rule, to obtain its posterior distribution. We derived a particle filter (PF) to compute Monte Carlo approximations of the posterior distribution, along with any other point estimate. To avoid the sample attrition issue, which often arises for time-invariant variables, the proposed PF employs a dynamical model based on that of West and Liu (2001). Besides matching the (previous analysis and current forecast) means and variances, as originally done in order to avoid the sample overdispertion over the time, we also constrained the inflation forecast particles to be positive, by generalizing the Gaussian noise of West and Liu (2001) to an inverse-Gamma noise whose parameters involve analytic expressions. The proposed scheme is easy to implement, and does not require the same number of particles for its EnKF and PF components. It is further potentially applicable to systems with large-dimensional states and moderately large-dimensional observations. Numerical experiments using the Lorenz-96 model demonstrated that the proposed method outperforms the benchmark Anderson (2007a) method in various experimental settings, including those where the algorithms use imperfect state and observation models.

The PF component of the proposed scheme could be extended to a more general sequential importance sampling algorithm involving arbitrary proposal sampling density. It could be also adapted to the case of spatio-temporal inflation vectors, for which, for instance, the PF could be replaced by the multiple PF (Ait-El-Fquih and Hoteit 2016), then compared to the existing spatio-temporal adaptive inflation schemes (e.g. Anderson 2009; Gharamti 2018; Bauser *et al.* 2018). This algorithm could also integrate the estimation of the localization radii and the observation noise variance. Finally, it would be of great interest to apply it to real-world data problems, with a focus on assessing its performances in both cases of inverse-Gamma and uniform inflation models.

M	10	20	30	40	50
A07 (a)	1.1107	1.0013	0.9697	0.9584	0.9494
PF-EnKF (a)	1.1213	0.9993	0.9731	0.9614	0.9527
A07 (b)	$7\ 10^{-4}$	$6.39\ 10^{-4}$	$6.19\ 10^{-4}$	$6.44\ 10^{-4}$	$6.3\ 10^{-4}$
PF-EnKF (b)	$3.48\ 10^{-4}$	$3.16\ 10^{-4}$	$3.31\ 10^{-4}$	$2.92\ 10^{-4}$	$3.04\ 10^{-4}$
A07 (c)	2.2544	2.0305	1.9663	1.9655	1.9406
PF-EnKF (c)	2.2076	2.0081	1.9561	1.9192	1.9228

Table 5. As in Tab. 1, but in the case of a perturbed observation noise variance.

f_o	2	4	6	8	10
A07 (a)	0.9945	1.0013	0.9937	0.9791	0.9694
PF-EnKF (a)	1.0021	0.9993	0.9955	0.9791	0.9675
A07 (b)	$7.56\ 10^{-4}$	$6.39\ 10^{-4}$	$6.86\ 10^{-4}$	$7.9\ 10^{-4}$	$9.01\ 10^{-4}$
PF-EnKF (b)	$3.09\ 10^{-4}$	$3.16\ 10^{-4}$	$3.87\ 10^{-4}$	$3.77\ 10^{-4}$	$3.66\ 10^{-4}$
A07 (c)	1.6252	2.0305	2.2771	2.5312	2.6995
PF-EnKF (c)	1.6009	2.0081	2.2667	2.5026	2.6836

Table 6. As in Tab. 2, but in the case of a perturbed observation noise variance.

Acknowledgements

Research reported in this publication was supported by King Abdullah University of Science and Technology (KAUST). The authors would like to thank the anonymous reviewers and François Desbouvries for the fruitful discussions about the resampling in the particle filter.

Appendix

Uniform inflation model

Imposing a positivity constraint through an uniform density within the framework of the revised West and Liu (2001) model ((25),(29)), implies using a transition density, $p(\lambda_n|\lambda_{n-1}, \mathbf{y}_{0:n-1})$, that is uniform with a positive support $[a, b]$, $\mathcal{U}[a, b]$. In this regard, the goal is to calculate a and b that satisfy (30). This can be achieved by equating the mean, $(a+b)/2$, and the variance, $(b-a)^2/12$, of the uniform density, $\mathcal{U}[a, b]$, with their counterparts in (30). One readily obtains,

$$\begin{cases} a &= g(\lambda_{n-1}) - \sqrt{3(\theta-\kappa^2)r^a_{n-1}}\ , \\ b &= g(\lambda_{n-1}) + \sqrt{3(\theta-\kappa^2)r^a_{n-1}}\ . \end{cases} \tag{36}$$

References

Ait-El-Fquih B, Desbouvries F. 2006. Kalman filtering in triplet Markov chains. *IEEE Transactions on Signal Processing* **54**(8): 2957–63.

Ait-El-Fquih B, Gharamti ME, Hoteit I. 2016. A Bayesian Consistent Dual Ensemble Kalman Filter for State-Parameter Estimation in Subsurface Hydrology. *Hydrology and Earth System Sciences* **20**: 3289–3307.

Ait-El-Fquih B, Hoteit I. 2016. A variational Bayesian multiple particle filtering scheme for large-dimensional systems. *IEEE Transactions on Signal Processing* **64**(20): 5409–22.

Ait-El-Fquih B, Hoteit I. 2018. An Efficient State-Parameter Filtering Scheme Combining Ensemble Kalman and Particle Filters. *Monthly Weather Review* **146**: 871–87.

Anderson JL. 2001. An ensemble adjustment Kalman filter for data assimilation. *Monthly Weather Review* **129**: 2884–2903.

Anderson JL. 2007a. An adaptive covariance inflation error correction algorithm for ensemble filters. *Tellus* **59A**: 210–24.

Anderson JL. 2007b. Exploring the need for localization in ensemble data assimilation using a hierarchical ensemble filter. *Physica D* **230**: 99–111.

Anderson JL. 2009. Spatially and temporally varying adaptive covariance inflation for ensemble filters. *Tellus* **61A**: 72–83.

Anderson JL, Anderson SL. 1999. A Monte Carlo implementation of the nonlinear filtering problem to produce ensemble assimilations and forecasts. *Monthly Weather Review* **127**(12): 2741–2758.

Bauser HH, Berg D, Klein O, Roth K. 2018. Inflation method for ensemble Kalman filter in soil hydrology. *Hydrology and Earth System Sciences Discuss.* doi:10.5194/hess-2018-74.

Bengtsson T, Bickel P, Li B. 2008. Curse-of-dimensionality revisited: Collapse of the particle filter in very large scale systems. *Probability and Statistics: Essays in Honor of David A. Freedman* **2**: 316–34.

Bishop C, Etherton B, Majumdar S. 2001. Adaptive sampling with the Ensemble Transform Kalman Filter. Part I: Theoretical aspects. *Monthly Weather Review* **129**: 420–36.

Bishop CH, Hodyss D. 2009a. Ensemble covariances adaptively localized with ECO-RAP. Part 1: Tests on simple errior models. *Tellus* **61A**: 84–96.

Bishop CH, Hodyss D. 2009b. Ensemble covariances adaptively localized with ECO-RAP. Part 2: A strategy for the atmosphere. *Tellus* **61A**: 97–111.

Bocquet M, Raanes M, Hannart A. 2015. Expanding the validity of the ensemble Kalman filter without the intrinsic need for inflation. *Nonlinear Processes in Geophysics* **22**: 645–62.

Brankart JM, Cosme E, Testut CE, Brasseur P, Verron J. 2010. Efficient adaptive error parameterizations for square root or ensemble Kalman filters: application to the control of ocean mesoscale signals. *Monthly Weather Review* **138**: 932–50.

Burgers G, van Leeuwen PJ, Evensen G. 1998. Analysis scheme in the ensemble kalman filter. *Monthly Weather Review* **126**: 1719–24.

Cappé O, Moulines E, Rydén T. 2005. *Inference in hidden Markov models*. Springer-Verlag.

Chui CK, Chen G. 1987. *Kalman Filtering*. Springer: Berlin.

Crisan D, Doucet A. 2002. A survey on convergence results on particle filtering methods for practitioners. *IEEE Transactions on Signal Processing* **50**(3): 736–46.

Dee DP. 2005. Bias and data assimilation. *Quarterly Journal of the Royal Meteorological Society* **131**: 3323–43.

Desroziers G, Berre L, Chapnik B, Poli P. 2005. Diagnosis of observation, background and analysis-error statistics in observation space. *Quarterly Journal of the Royal Meteorological Society* **131**: 3385–96.

Dimet FXL, Talagrand O. 1986. Variational algorithms for analysis and assimilation of meteorogical observations: Theoretical aspects. *Tellus* **38A**: 97–110.

Doucet A, de Freitas N, Gordon N (eds). 2001. *Sequential monte carlo methods in practice*. Statistics for Engineering and Information Science, Springer Verlag: New York.

Duan D, Tandeo P, Pulido M, Ait-El-Fquih B, Chonavel T, Hoteit I. 2017. Estimating model-error covariances in nonlinear state-space models using Kalman smoothing and the expectation-maximization algorithm. *Quarterly Journal of the Royal Meteorological Society* **143**: 1877–85.

Edwards CA, Moore AM, Hoteit I, Cornuelle BD. 2015. Regional Ocean Data Assimilation. *Annual Review of Marine Science* **7**: 21–42.

Evensen G. 2006. *Data Assimilation: The Ensemble Kalman Filter*. New York: Springer.

Frei M. 2013. Ensemble Kalman Filtering and Generalizations. PhD thesis, ETH-Zürich.

Frei M, Künsch H. 2012. Sequential State and Observation Noise Covariance Estimation Using Combined Ensemble Kalman and Particle Filters. *Monthly Weather Review* **140**: 1476–95, doi:10.1175/MWR-D-10-05088.1.

Frei M, Künsch HR. 2013. Mixture ensemble Kalman filters. *Computational Statistics and Data Analysis* **58**: 127–38.

Furrer R, Bengtsson T. 2007. Estimation of high-dimensional prior and posterior covariance matrices in Kalman filter variants. *Journal of Multivariate Analysis* **98**(2): 227–55.

Gaspari G, Cohn SE. 1999. Construction of correlation functions in two and three dimensions. *Quarterly Journal of the Royal Meteorological Society* **125**(554): 723–757.

Gharamti ME. 2018. Enhanced adaptive inflation algorithm for ensemble filters. *Monthly Weather Review* **146**: 623–40.

Gharamti ME, Ait-El-Fquih B, Hoteit I. 2015. An iterative ensemble Kalman filter with one-step-ahead smoothing for state-parameters estimation of contaminant transport models. *Journal of Hydrology* **527**: 442–57.

Gordon NJ, Salmond DJ, Smith AFM. 1993. Novel approach to nonlinear/ non-Gaussian Bayesian state estimation. *IEE Proceedings - F* **140**: 107–113.

Hamill TM, Snyder C. 2000. A hybrid ensemble Kalman filter–3D variational analysis scheme. *Monthly Weather Review* **128**(8): 2905–2919.

Hamill TM, Whitaker JS. 2010. What constrains spread growth in forecasts initialized from ensemble Kalman filters? *Monthly Weather Review* **139**: 117–31.

Hoteit I, Luo X, Bocquet M, Kohl A, Ait-El-Fquih B. 2018. *New frontiers in operational oceanography*, ch. 17: Data assimilation in oceanography: current status and new directions. GODAE Ocean View, pp. 465–512.

Hoteit I, Luo X, Pham D. 2012. Particle Kalman Filtering: A Nonlinear Bayesian Framework for Ensemble Kalman Filters. *Monthly Weather Review* **140**: 528–42.

Hoteit I, Pham DT, Gharamti ME, Luo X. 2015. Mitigating observation perturbation sampling errors in the stochastic EnKF. *Monthly Weather Review* **143**: 2918–36.

Hoteit I, Pham DT, Triantafyllou G, Korres G. 2008. A new approximate solution of the optimal nonlinear filter for data assimilation in meteorology and oceanography. *Monthly Weather Review* **136**(1): 317–334.

Houtekamer PL, Mitchell HL. 1998. Data assimilation using an ensemble Kalman filter technique. *Monthly Weather Review* **126**: 796–811.

Houtekamer PL, Mitchell HL. 2005. Ensemble Kalman filtering. *Quarterly Journal of the Royal Meteorological Society* **131**: 3269–89.

Jazwinski AH. 1970. *Stochastic processes and filtering theory*, *Mathematics in Science and Engineering*, vol. 64. Academic Press: San Diego.

Kalman RE. 1960. A new approach to linear filtering and prediction problems. *Transactions of the ASME–Journal of Basic Engineering, Series D* **82**(1): 35–45.

Kivman GA. 2003. Sequential parameter estimation for stochastic systems. *Nonlinear Processes in Geophysics* **10**(3): 253–59.

Kotsuki S, Ota Y, Miyoshi T. 2017. Adaptive covariance relaxation methods for ensemble data assimilation: experiments in the real atmosphere. *Quarterly Journal of the Royal Meteorological Society* **143**: 2001–15.

Künsch H. 2001. State space and hidden markov models. In: *Complex Stochastic Systems*, Barndorff-Nielsen OE, Cox DR, Klüppelberg C (eds), ch. 3, CRC Press, pp. 109–173.

Lamberti R, Petetin Y, Desbouvries F, Septier F. 2017. Independent Resampling Sequential Monte Carlo Algorithms. *IEEE Transactions on Signal Processing* **65**(20): 5318–33.

Li B, Kalnay E, Miyoshi T. 2009. Simultaneous estimation of covariance inflation and observation errors within an ensemble Kalman filter. *Quarterly Journal of the Royal Meteorological Society* **135**: 523–33.

Liang X, Zheng X, Zhang S, Wu G, Dai Y, Li Y. 2012. Maximum likelihood estimation of inflation factors on error covariance matrices for ensemble Kalman filter assimilation. *Quarterly Journal of the Royal Meteorological Society* **128**: 263–73.

[illegible] B, Ait-El-Fquih B, Hoteit I. 2015. Efficient Kernel-Based Ensemble Gaussian Mixture Filtering. *Monthly Weather Review* **144**: 781–800.

[illegible]u JS, Chen R. 1998. Sequential monte carlo methods for dynamic systems. *Journal of the American Statistical Association* **93**(443): 1032–44.

Lorenz EN, Emanuel KA. 1998. Optimal sites for supplementary weather observations: Simulation with a small model. *Journal of the Atmospheric Sciences* **55**(3): 399–414.

Luo X, Hoteit I. 2011. Robust ensemble filtering and its relation to covariance inflation in the ensemble Kalman filter. *Monthly Weather Review* **139**: 3938–53.

Mitchell HL, Houtekamer PL. 2000. An adaptive ensemble Kalman filter. *Monthly Weather Review* **128**: 416–33.

Miyoshi T. 2011. The gaussian approach to adaptive covariance inflation and its implementation with the local ensemble transform Kalman filter. *Monthly Weather Review* **139**: 1519–35.

Raanes PN, Bocquet M, Carrassi A. 2018. Adaptive covariance inflation in the ensemble Kalman filter by Gaussian scale mixtures. *Quarterly Journal of the Royal Meteorological Society* **145**: 53–75.

Raboudi NF, Ait-El-Fquih B, Hoteit I. 2018. Ensemble Kalman Filtering with One-Step-Ahead Smoothing. *Monthly Weather Review* **146**: 561–81.

R[illegible]chle RH. 2008. Data assimilation methods in the Earth sciences. *Advances in Water Resources* **31**: 1411–18.

R[illegible]obert C. 2007. *The Bayesian Choice: From Decision-Theoretic Foundations to Computational Implementation*. Springer Science & Business Media: New York.

Rubin D. 1988. Using the SIR algorithm to simulate posterior distributions. In: *Bayesian Statistics*, vol. 3, Bernardo J, DeGroot M, Lindley D, Smith A (eds), Oxford University Press, pp. 395–402.

Sakov P, Haussaire JM, Bocquet M. 2018. An iterative ensemble Kalman filter in the presence of additive model error. *Quarterly Journal of the Royal Meteorological Society* **144**(713): 1297–1309.

Smidl V, Hofman R. 2011. Marginalized particle filtering framework for tuning of ensemble filters. *Monthly Weather Review* **139**: 3589–99.

Smidl V, Quinn A. 2008. Variational Bayesian Filtering. *IEEE Transactions on Signal Processing* **56**(10): 5020–5030.

Snyder C, Bengtsson T, Bickel P, Anderson J. 2008. Obstacles To High-Dimensional Particle Filtering. *Monthly Weather Review* **136**(12): 4629–40.

Song H, Hoteit I, Cornuelle B, Subramanian A. 2010. An adaptive approach to mitigate background covariance limitations in the ensemble Kalman filter. *Monthly Weather Review* **138**: 2825–45.

Tippett M, Anderson J, Bishop C, Hamill T, Whitaker J. 2003. Ensemble square root filters. *Monthly Weather Review* **131**(7): 1485–1490.

van Leeuwen PJ. 2009. Particle Filtering in Geophysical Systems. *Monthly Weather Review* **137**(12): 4089–4114.

van Trees H. 1968. *Detection, Estimation, and Modulation Theory : Part I*. John wiley and Sons: New York.

Wang X, Bishop CH. 2003. A comparison of breeding and ensemble transform Kalman filter ensemble forecast schemes. *Journal of the Atmospheric Sciences* **60**: 1140–58.

West M, Liu J. 2001. Combined parameter and state estimation in simulation-based filtering. In: *Sequential Monte Carlo Methods in Practice*, Doucet A, de Freitas N, Gordon N (eds), Springer, pp. 197–223.

Whitaker JS, Hamill HT, Wei X, Song Y, Toth Z. 2008. Ensemble data assimilation with the NCEP global forecast system. *Monthly Weather Review* **136**: 463–81.

Whitaker JS, Hamill TM. 2012. Evaluating methods to account for system errors in ensemble data assimilation. *Monthly Weather Review* **140**: 3078–89.

Whitaker JS, Hamill TS. 2002. Ensemble Data Assimilation without Perturbed Observations. *Monthly Weather Review* **130**: 1913–24.

Zheng X. 2009. An adaptive estimation of forecast error covariance parameters for Kalman filtering data assimilation. *Advances in Atmospheric Sciences* **26**: 154–60.

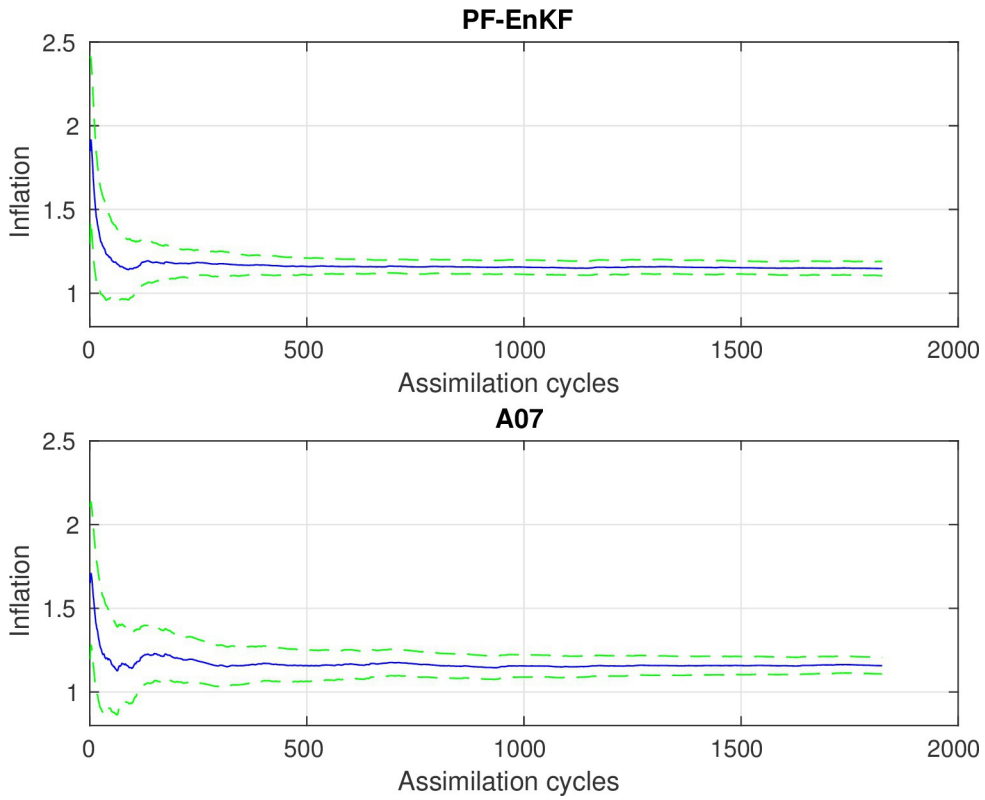

figure1.eps

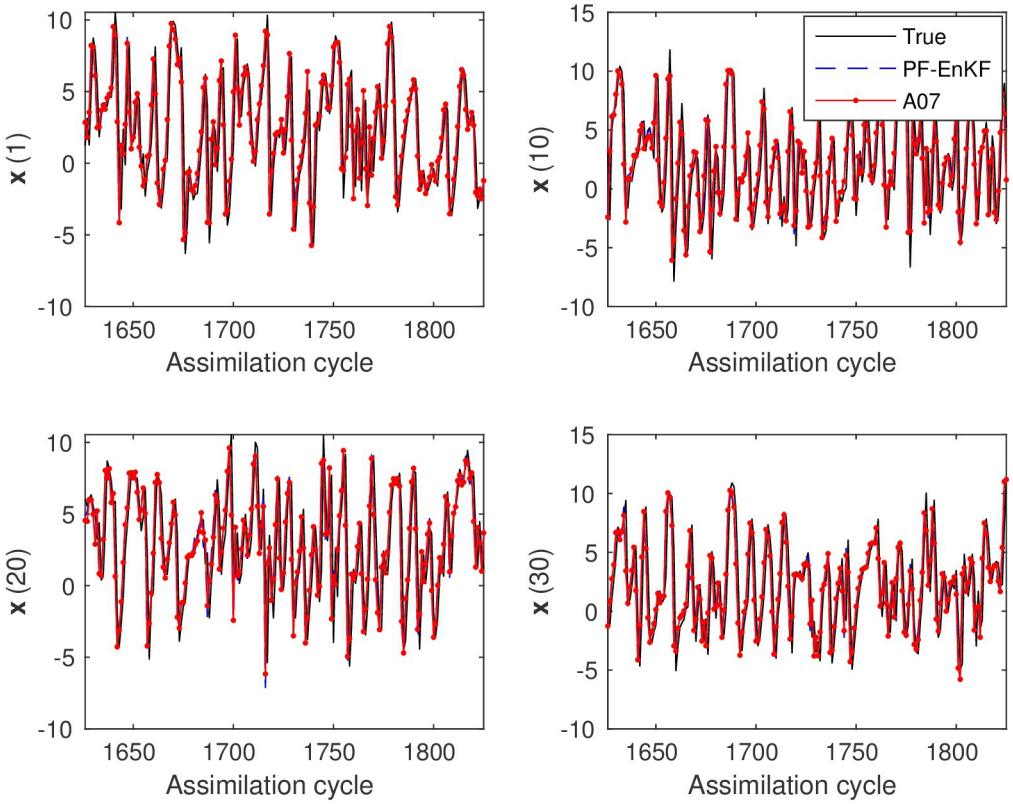

figure2.eps

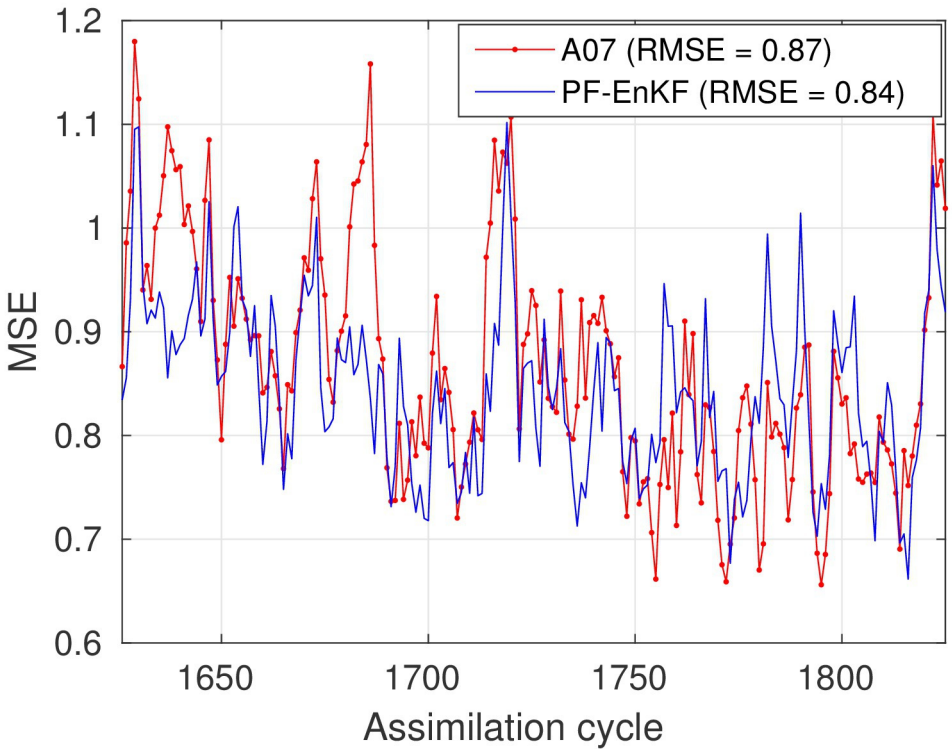

figure3.eps

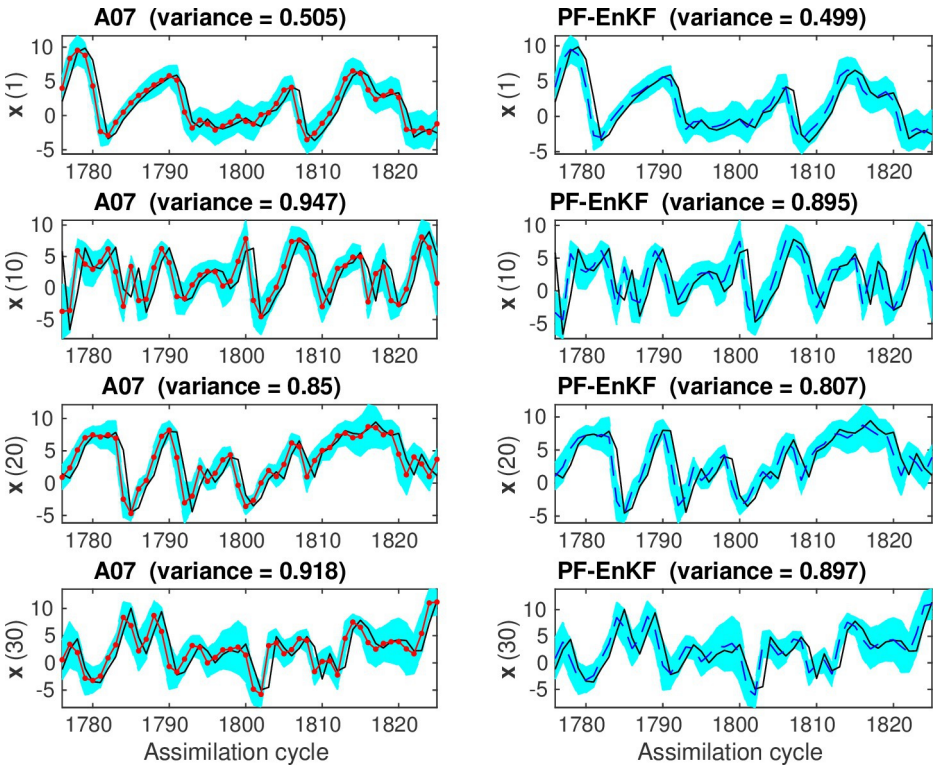

figure4.eps